Effects of TFT mobility variation in the threshold voltage compensation circuit of the OLED display

YoungHa Sohn, GeumJu Moon, KwangHyun Choi, YongSang Kim & KeeChan Park

Taylor & Francis
Taylor & Francis Group

Effects of TFT mobility variation in the threshold voltage compensation circuit of the OLED display

YoungHa Sohn[a], GeumJu Moon[a], KwangHyun Choi[a], YongSang Kim[b] and KeeChan Park[a]

[a]Department of Electronics Engineering, Konkuk University, Seoul, Republic of Korea; [b]Department of Electrical & Electronic Engineering, Sungkyunkwan University, Suwon, Republic of Korea

ABSTRACT

A pixel circuit that compensates for the non-uniform thin-film transistor (TFT) characteristics across a display panel is inevitably used in the organic light-emitting diode (OLED) display to exhibit uniform brightness. The existing pixel circuits aim to compensate only for the non-uniformity of the threshold voltage (V_{th}). They do not compensate for the deviation of the other parameters, such as the mobility and the subthreshold swing. In this study, how the OLED current changes when the mobility of a TFT in the V_{th} compensation circuit increases was examined. If the mobility increases, the enhanced drain current drives the TFT into a deeper subthreshold mode during the V_{th} compensation phase, and the $|V_{GS}|$ of the TFT decreases compared with the normal mobility case. The resultant OLED current, however, can be higher or lower than the normal mobility case depending on the gray level because the effects of the current increase due to the higher mobility and of the current decrease due to the reduced $|V_{GS}|$ appear simultaneously but differently depending on the V_{GS} value of the TFT. The analysis results show that the OLED current increases for the high gray level but decreases for the low gray level. It remains almost unaffected by the mobility increase for the mid-gray level.

1. Introduction

The organic light-emitting diode (OLED) displays recently replaced the liquid crystal displays (LCDs) for mobile devices such as smartphones, owing to the high flexibility, better image quality, and lower power consumption of OLED. It is troublesome, however, to exhibit uniform brightness on the OLED display panel compared with the LCD because the brightness of the OLED pixel is determined by the current in each pixel rather than by the voltage stored in a capacitor, which is the method used in the LCD. The pixel of the OLED display also stores the data voltage supplied by a driver IC, which is very uniform. In the case of the OLED display; however, an additional conversion process from the data voltage to the pixel current is required. This voltage-to-current conversion is carried out by a thin-film transistor (TFT) in each pixel. In the process of conversion, severe mura appears when the characteristics of the TFT are not sufficiently uniform. Therefore, a pixel circuit is needed to compensate for the TFT non-uniformity and to have a uniform voltage-to-brightness relation.

For example, in the case of the low-temperature polycrystalline silicon (LTPS) TFT, the device parameters such as the carrier mobility, threshold voltage (V_{th}), and subthreshold swing vary depending on the random distribution of the grain boundaries in the polycrystalline silicon (poly-Si) film [1,2]. The conventional pixel circuits are designed to compensate only for the variation of the V_{th} of the TFT [3–8]. The V_{th} compensation is more effective than the compensation of other parameters, such as the mobility and subthreshold swing, because the OLED-driving TFT operates around the threshold point to realize a high contrast ratio, and the variation of V_{th} critically affects the TFT current in this bias range. The mobility variation, however, may also influence the uniformity of the TFT current, but the effects of the mobility variation on the TFT current in the V_{th} compensation circuit have not yet been investigated. Reported in this paper is how the compensated-for OLED current varies when the mobility of the TFT increases in the conventional V_{th} compensation circuit.

CONTACT KeeChan Park ✉ keechan@konkuk.ac.kr Department of Electronics Engineering, Konkuk University, Seoul143-701, Republic of Korea

2. Operation of the V_{th} compensation pixel circuit

Figure 1 shows Choi's 6T1C V_{th} compensation circuit, which was used in the analysis [1]. This circuit has been used in the Samsung smartphones for nearly 10 years. The operation of the pixel circuit consists of three phases, as shown in the timing diagram in Figure 1(b). First, in the initializing phase, the OLED-driving TFT M1 is turned on by the initialization voltage (VI), which is supplied through M4, as shown in Figure 2(a). Therefore, the previous data stored in the capacitor are deleted. Then, in the programing phase, a new data voltage is supplied to the source terminal of M1 through M2, as shown in Figure 2(b). During this phase, current flows through M1 because the gate potential of M1 is VI, which is sufficiently lower than the data voltage that is the source potential of M1. The current that flows through M1 raises the potential of the gate node of M1. At the end of the programing phase, the V_{GS} of M1 approaches the V_{th} of M1, and the current decreases sharply. Accordingly, the gate potential of M1 becomes $V_{data} + V_{th}$. Finally, it turns into the emission phase, and the V_{GS} of M1 becomes $V_{data} + V_{th} - VDD$, which is stored in the storage capacitor, as shown in Figure 2(c). As a result, the OLED current that is identical to the current of M1 is determined independently of the V_{th} of M1, as expressed by Equation (1). Other V_{th} compensation circuits work in a similar way [3–8].

$$I_{OLED} = \frac{1}{2}k\mu(V_{GS} - V_{th})^2 = \frac{1}{2}k\mu(V_{data} - VDD)^2. \tag{1}$$

Figure 3 shows the waveforms of gate voltage V_G and source voltage V_S of M1 during the operation shown in Figure 2. It should be noted that V_G (red solid and black dashed lines) approaches V_S (blue dash-dot-dot line) with a voltage gap corresponding to the V_{th} of M1 during the programing and compensation phase. At the end of this phase, the speed of V_G change slows down because the current of M1 decreases as it enters the sub-threshold mode. In Figure 3, it can also be verified that the rate of V_G change depends on the carrier mobility of M1. V_G changes faster when the mobility is higher (red solid line). From this result, it can be expected that mobility deviation may affect the compensated-for V_{GS} value.

3. Mobility parameters in the spice model

To investigate the effects of TFT mobility on the V_{th} compensation circuit, a SmartSpice simulator and the Rensselaer Polytechnic Institute (RPI) poly-Si TFT model (level 36) were used. Table 1 shows the device parameters constituting the TFT model. These parameters determine the current-to-voltage characteristics of the device synthetically according to the bias condition. In this analysis, only three parameters were controlled: MU0, MU1, and MUS, which are directly related to the mobility of the TFT. MU0 means high-field mobility and influences the current of TFT when V_{GS} is high. MU1 means low-field mobility and influences the current of TFT when V_{GS} is close to V_{th}. MUS means subthreshold mobility and influences the current of TFT in the subthreshold mode.

How these three parameters affect the transfer characteristics of the TFT model was examined. Figure 4 shows the transfer characteristics when MU0, MU1, and MUS are doubled, respectively. The simulation condition was $V_{DS} = -10$ V, and the channel width and length of the TFT were 2 and 10 μm, respectively. Each parameter increased a different part of the transfer characteristics. When only MU0 was doubled, the TFT current noticeably increased for $V_{GS} < -3$ V, and by as much as 60%
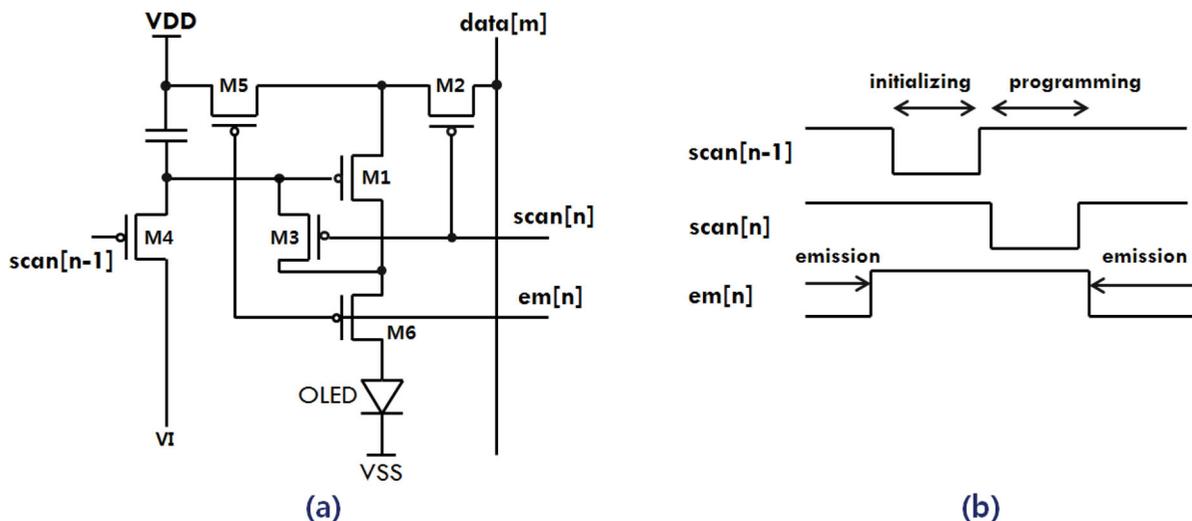
Figure 1. (a) PMOS 6T1C Vth compensation pixel circuit in Ref. [1]; (b) its timing diagram.
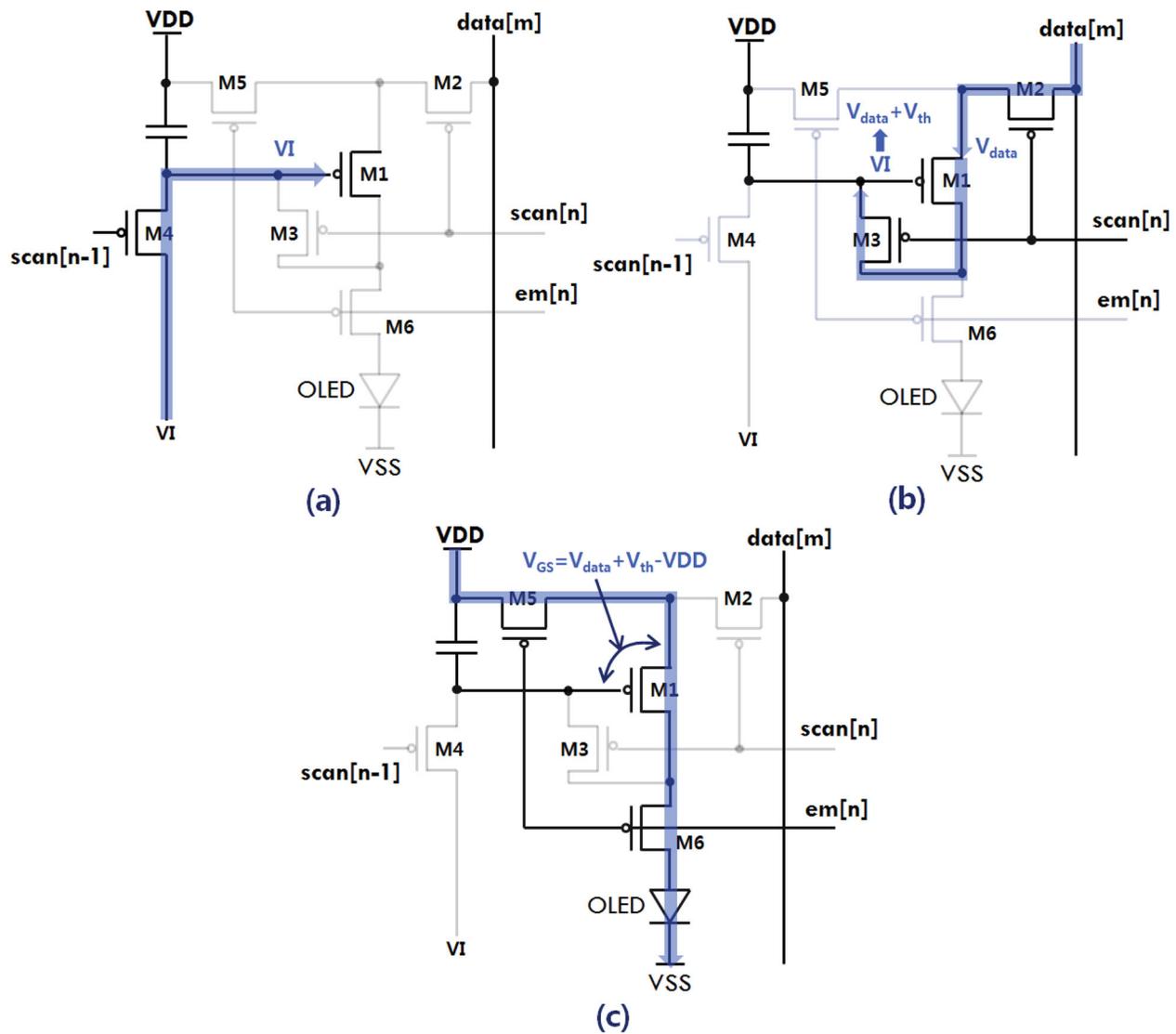
Figure 2. (a) Initializing phase, (b) programing phase, and (c) emission phase of the 6T1C circuit operation process.
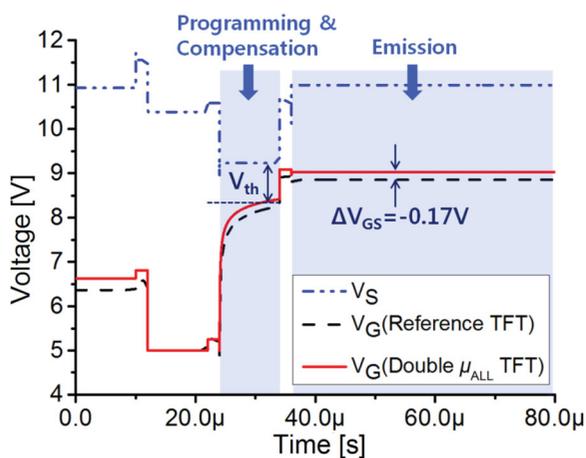
Figure 3. Waveforms of the gate and source voltages of M1 TFT during the operation phases for the different mobility cases.

Table 1. RPI poly-Si TFT model parameters for spice simulation.

Parameter	Value	Parameter	Value	Parameter	Value
TNOM	27	TOX	1E−7	VON	0
VTO	−0.57	VFB	0	CGSO	3E−10
DVT	0	VKINK	10	CGDO	3E−10
MU1	1E−3	MMU	2.6	MUS	1
MU0	50	MK	1.3	BT	1E−7
RD	1.5E+3	RS	1.5E+3	DELTA	4
BLK	1.9E−6	DD	9E−8	ETA	3.6
DG	2E−7	EB	0.55	ASAT	1
I0	6	I00	150	LASAT	0
AT	3E−9	DASAT	0	RSH	1.5E+3
LKINK	1.9E−6				

for $V_{GS} < -9$ V, as shown in Figure 4(a). As can be seen in Figure 4(b), when only MU1 was doubled, the TFT current increased for the V_{GS} close to the V_{th}, and the maximum increase was 60% for the V_{GS} slightly above
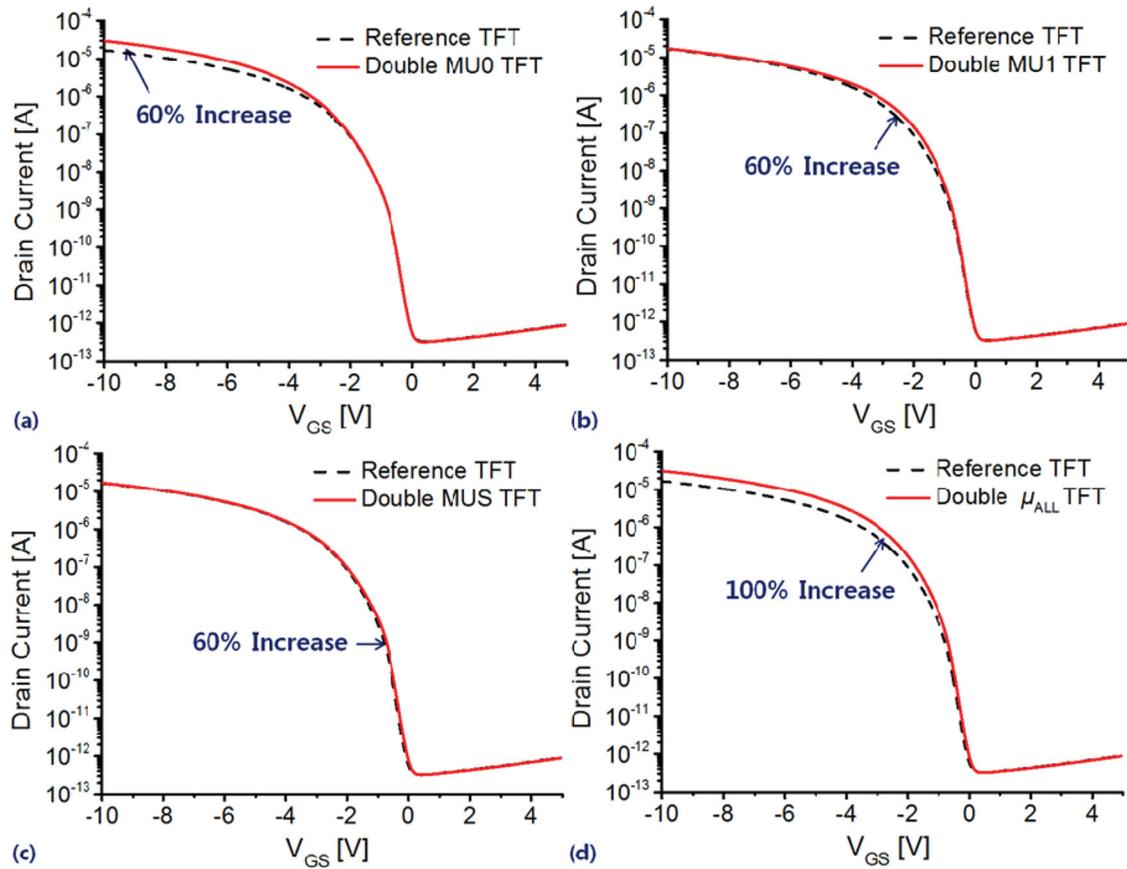
Figure 4. Transfer characteristics of the TFT models for (a) high-field mobility (MU0) doubling, (b) low-field mobility (MU1) doubling, (c) subthreshold mobility (MUS) doubling, and (d) all the mobilities' (MU0, MU1, and MUS) doubling when $V_{DS} = -10\,$V and TFT's $W/L = 2\,\mu$m/$10\,\mu$m.

the V_{th}. As shown in Figure 4(c), when only MUS was doubled, only the subthreshold current increased, and by about 60%. When all the three parameters were doubled at the same time, the overall TFT current increased by more than 80%, except for the leakage current, as shown in Figure 4(d). The maximum increase of the TFT current was about 100% for the V_{GS} slightly above the V_{th}. In the following analysis, only the case in which all the three mobility parameters were doubled were considered because the overall current could increase if the poly-Si film quality of the fabricated TFT was better than the reference.

4. Results

As shown in Figure 3, during the programing and compensation phase, the V_G of the double-mobility TFT rose faster than the V_G of the reference TFT because the current of the double-mobility TFT was higher. At the end of this phase, the difference between the two V_G's was about 0.17 V. This difference, in principle, was almost independent of the data voltage (i.e. the gray level) because the V_{GS} of M1 approached V_{th} irrespective of the data

voltage. In the next phase, the V_S of M1 for both cases became VDD, and the difference of the V_{GS} between the different mobility cases remained as 0.17 V. In other words, the absolute value of V_{GS}, $|V_{GS}|$, was smaller during the emission phase, when the mobility was higher.

Figure 5 shows how the OLED current changed when the mobility was doubled compared with the reference case. As mentioned earlier, the difference of $|V_{GS.M1}|$ between the two cases had an almost constant value (0.17 V) in all the OLED current cases (1, 10, and 100 nA). The OLED current of the double-mobility case, however, could be larger or smaller compared with the reference case because the mobility as well as the V_{GS} determined the current simultaneously according to Equation (1). When the OLED current of the reference case was 10 nA, there was little difference, although the mobility was doubled. The effect of the mobility increase was canceled out by the $|V_{GS.M1}|$ decrease. In the case of 1 nA, however, although the difference of $|V_{GS.M1}|$ was the same (0.17 V), the current of the double-mobility case decreased by more than 40% compared with the reference case because the current-increasing effect due to the mobility increase was smaller than the effect of the
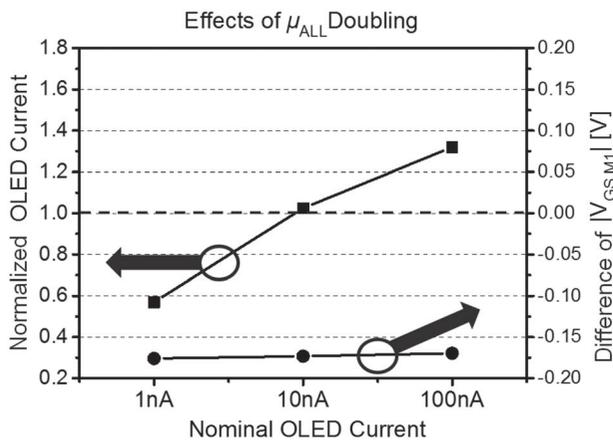
Figure 5. Effects of all the mobilities' doubling on the programed $|V_{GS.M1}|$ values, and resultant OLED currents vs. the various target currents.

$|V_{GS.M1}|$ decrease. In contrast, in the case of 100 nA, the difference of $|V_{GS.M1}|$ was also 0.17 V, but the current increased by about 32% because the current-increasing effect due to the mobility increase was larger than the effect of the $|V_{GS.M1}|$ decrease.

Figure 6 shows the transfer characteristics of M1 for the cases when the OLED current was 1, 10, and 100 nA. For the low gray level (1 nA, Figure 6(a)), the TFT was in the subthreshold mode, and the effect of the $|V_{GS.M1}|$ decrease was stronger (exponentially proportional) than the effect of the mobility increase. Therefore, the current decreased for the 1 nA case. For the mid-gray level (10 nA, Figure 6(b)), the TFT was slightly above the threshold condition, and the effect of the mobility increase was almost compensated for by the $|V_{GS.M1}|$ decrease during the V_{th} compensation phase. For the high gray level (100 nA, Figure 6(c)), the bias condition of the TFT was sufficiently above the threshold voltage, and the effect of the mobility increase was stronger than that of the $|V_{GS.M1}|$ decrease because the current was proportional merely to the square of V_{GS} (not in the exponential proportion). Accordingly, the current increased for the 100 nA case.

5. Conclusion

The pixel current of the OLED display employing a V_{th} compensation circuit can be affected by the mobility variation of the TFTs. The compensated-for OLED current tends to decrease for the low gray level but to increase for the high gray level when the mobility increases because the effect of the current increase due to the higher mobility and that of the current decrease due to the reduced
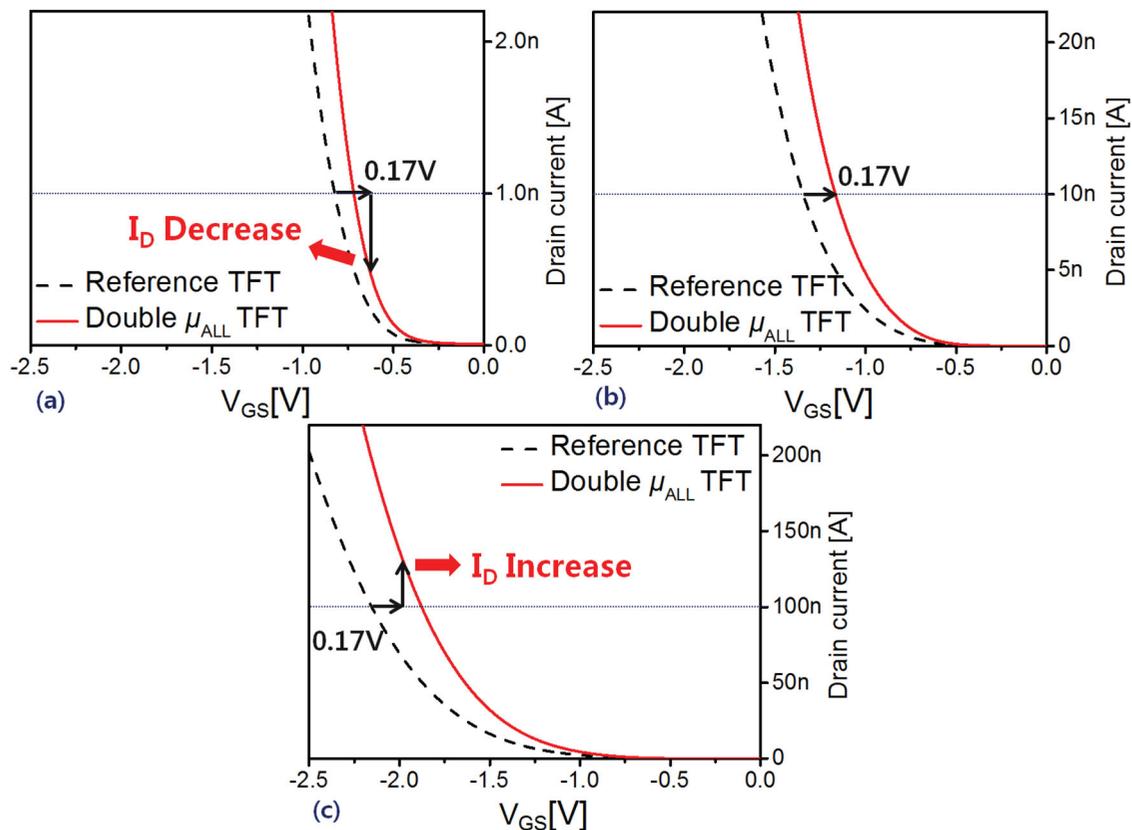
Figure 6. Different effects of the programed $|V_{GS.M1}|$ decrease on the OLED currents for various target currents: (a) 1 nA; (b) 10 nA; and (c) 100 nA.

$|V_{GS}|$ during the emission phase appear simultaneously but differently depending on the V_{GS} value of the TFT. When the TFT is in the deep subthreshold mode, the effect of a reduced $|V_{GS}|$ is stronger than that of mobility increase. The effect of mobility increase is stronger, however, than that of $|V_{GS}|$ decrease when the TFT is sufficiently above the threshold point.

Reported in this paper is only the effect of double-mobility increase on the operation of the V_{th} compensation pixel circuit. The same trend of current variation was also verified, however, when the mobility increase is less than twofold, although it is not presented in this paper.

Disclosure statement

No potential conflict of interest was reported by the author.

Notes on contributors

YoungHa Sohn received his B.S. Electronics Engineering degree from Konkuk University in 2015 and is now an M.S. candidate in the same university. His main interests are characterization of LTPS TFTs, the pixel compensation circuit of the OLED display, and the driving circuit of the display panel.

GeumJu Moon received his B.S. Electronics Engineering degree from Konkuk University in 2015 and is now an M.S. candidate in the same university. His main interests are analyses of the TFT characteristics and of power devices such as IGBT.

KwangHyun Choi received his B.S. Nano-Science and Mechanical Engineering degree from Konkuk University Glocal Campus in 2016 and is now an M.S. candidate in Konkuk University, Seoul. He has been researching on the analysis of the driving circuit for displays, and on designing the layout of a pixel circuit for mobile displays.

YongSang Kim received his B.S., M.S. and Ph.D. Electrical Engineering degrees from Seoul National University, Seoul, South Korea in 1988, 1990, and 1994, respectively. He was a professor at Myongji University from 1995 to 2013, and at Sungkyunkwan University from 2013. His research interests are the organic-transistor-based biosensor, organic solar cells, oxide TFTs, and solution-processing technologies for organic electronic devices.

KeeChan Park received his B.S., M.S. and Ph.D. Electrical Engineering degrees in 1997, 1999, and 2003, respectively, from Seoul National University, Seoul, South Korea. He worked as a senior engineer at Samsung Electronics from 2003 to 2007. From 2007 to the present, he has been a professor at Konkuk University. His research areas include the design of display panels, circuit integration using TFTs, and device characterization.

References

[1] S.H. Jang, B.T. Son, S.H. Choi, D.J. Kim, G.S. Kim and M.H. Yoo, SID Symp. Dig. Tech. Pap. **47**, 1162 (2016).
[2] C.W. Yang and P. Su, IEEE Trans. Electron Dev. **61**, 1211 (2014).
[3] S.M. Choi, O.K. Kwon, N. Komiya and H.K. Chung, IDW **4**, 535 (2003).
[4] Y.W. Kim, W.K. Kwak, J.Y. Lee, W.S. Choi, K.Y. Lee, S.C. Kim and E.J. Yoo, SID Symp. Dig. Tech. Pap. **40**, 85 (2009).
[5] J.H. Lee, J.H. Kim and M.K. Han, IEEE Electron Dev. Lett. **26**, 897 (2005).
[6] C.L. Lin and Y.C. Chen, IEEE Electron Dev. Lett. **28**, 129 (2007).
[7] H.Y. Lu, T.C. Chang, Y.H. Tai, P.T. Liu and S. Chi, J. Display Technol. **3**, 398 (2007).
[8] D.W. Park, C.K. Kang, Y.S. Park, B.Y. Chung, K.H. Chung, K.N. Kim, B.H. Kim and S.S. Kim, J. SID **19**, 329 (2011).